3446

3D-CAIPI-BUDA and Joint Hankel Low-Rank Reconstruction Enable Rapid and Distortion-free High-Resolution T2* Mapping and QSM

Zhifeng Chen[1,2,3], Congyu Liao[4], Xiaozhi Cao[4], Benedikt A Poser[5], Zhongbiao Xu[6], Wei-Ching Lo[7], Manyi Wen[8], Jaejin Cho[1], Qiyuan Tian[1], Yaohui Wang[9], Yanqiu Feng[3], Wufan Chen[3], Ling Xia[10], Feng Liu[11], and Berkin Bilgic[1,2]

[1]Athinoula A. Martinos Center for Biomedical Imaging, Massachusetts General Hospital, Charlestown, MA, United States, [2]Department of Radiology, Harvard Medical School, Charlestown, MA, United States, [3]School of Biomedical Engineering, Guangdong Provincial Key Laboratory of Medical Image Processing, Southern Medical University, Guangzhou, China, [4]Department of Radiology, Stanford University, Stanford, CA, United States, [5]Maastricht Brain Imaging Center, Faculty of Psychology and Neuroscience, University of Maastricht, Maastricht, Netherlands, [6]Department of Radiotherapy, Cancer Center, Guangdong Provincial People's Hospital & Guangdong Academy of Medical Science, Guangzhou, China, [7]Siemens Medical Solutions, Boston, MA, United States, [8]Department of Chemical Pathology, The Chinese University of Hong Kong, Hong Kong, China, [9]Division of Superconducting Magnet Science and Technology, Institute of Electrical Engineering, Chinese Academy of Sciences, Beijing, China, [10]Department of Biomedical Engineering, Zhejiang University, Hangzhou, China, [11]School of Information Technology and Electrical Engineering, The University of Queensland, Brisbane, Australia

Synopsis

Quantitative imaging has been very useful in neuroscientific and clinical applications, including glioma, tumor diagnosis and prognosis, brain maturation, and Alzheimer's disease. EPI is a powerful tool for quantitative imaging owing to its extremely fast acquisition. This work aims to develop a distortion-free, blip-up/down acquisition (BUDA) 3D-EPI with controlled aliasing in parallel imaging (CAIPI) sampling and joint Hankel low-rank image reconstruction for fast and robust multi-contrast high-resolution whole-brain imaging. The developed technique could generate distortion-free high-resolution whole-brain T2* mapping and quantitative susceptibility mapping in 47s at $1.1\times1.1\times1$ mm^3 resolution.

Purpose

Quantitative MRI has gained recent attention owing to its emerging neuroscientific and clinical applications[1–3]. Echo planar imaging (EPI) is a rapid encoding technique that has played an essential role in functional and diffusion MRI[4,5], quantitative imaging[1,6,7], and susceptibility mapping[8]. Despite the fast acquisition speed, distortion and voxel pile-ups have remained an open problem[7,9], and led to technical developments that aimed to improve the geometric fidelity of EPI[5,6,10–12].

In this work, we propose to combine 3D blip-up/down acquisition (BUDA)[13] with CAIPI[14,15] sampling and joint Hankel low-rank reconstruction to obtain high-resolution, distortion-free, multi-contrast images. The results demonstrate improved image quality by incorporating staggered CAIPI sampling across the multi-shot data to provide complementary information. For *in vivo* T2* mapping, high agreement between the proposed 3D-BUDA and standard multi-echo GRE was observed, as corroborated by Bland-Altman analysis. Further, the ability to perform QSM is demonstrated from the same set of distortion-free multi-echo EPI data.

Method & Experiments

Novel acquisition: The proposed multi-echo 3D-BUDA sequence diagram is presented in Figure 1. Blip-up/down phase encoding is implemented for each echo (yellow and green blips in G_{PE}), respectively. High $R_{inplane}$ acceleration enabled by multi-shot acquisition allowed for inserting three echoes with adequate echo times for T2* mapping and QSM.

CAIPI strategy is employed for improving the conditioning of the image reconstruction[14,15]. In this work, CAIPI is performed between the blip-up/down shots, as shown in Figure 3.

Novel reconstruction: A joint reconstruction approach is proposed and demonstrated using multi-echo multi-shot 3D-BUDA GRE-EPI data, as shown in Figure 2:

$$\tilde{I} = \arg\min_{I} \sum_{t,n} \|M_{t,n}F_{t,n}ECI_{t,n} - d_{t,n}\|_F^2 + \lambda\|H(I)\|_*$$

Where t is the shot count, n represents the echo index. $M_{t,n}$ and $F_{t,n}$ are the sampling mask and Fourier transform operator (t^{th} shot, n^{th} echo), respectively. C represents the coil sensitivity maps; I is the to-be-restored images, and $d_{t,n}$ stands for the acquired under-sampled k-space data. E is the B_0 field map generated by TOPUP using FSL on interim blip-up and -down separate reconstructions (http://fsl.fmrib.ox.ac.uk/fsl) [16]. $\|H(I)\|_*$ denotes the Hankel matrix along both shot and echo dimensions for multi-echo multi-shot data[17,18]. It enforces local k-space neighborhoods (of size 9×9×9), extended across all echoes/contrasts in the shot dimension, to have structured low-rankness property. A POCS-like algorithm[19] was employed to solve the above equation with a stopping criterion of root mean square error (RMSE) < 1% between consecutive iterations.

Data acquisition: *In vivo* multi-echo, multi-shot 3D-BUDA experiments were performed on a 3T scanner (Magnetom Tim Trio; Siemens Healthineers) with a 32-ch head coil. Imaging parameters include: $R_{inplane}$=8, TR=86ms, TE={18, 43.17, 68.34}ms, FA 19° (Ernst angle), FOV 220×220×128 mm^3, spatial resolution=1.1×1.1×1 mm^3.

T2* maps were obtained using Bloch dictionary matching[20]. The dictionary comprised signal evolution curves of T2* values were set as [1:1:100, 101:2:200, 201:3:300] ms.

QSM was estimated using a nonlinear dipole inversion (NDI)[21,22]:

$$\tilde{\chi} = arg\min_{\chi} \left\| W\left(e^{iF^{-1}DF\chi} - e^{i\phi}\right)\right\|_2^2$$

where $\boldsymbol{W}$ is magnitude weighting, D and F are the dipole kernel and 3D-DFT operator. ϕ is the tissue phase, χ is the to-be-calculated susceptibility map.

All computations were implemented in MATLAB; code/data will be found on Github(https://github.com/zjuczf168/zjuczf168/blob/main/3D-BUDA) upon publication of this work.

Data Analysis

"Fully sampled" multi-shot multi-echo BUDA data were used as a reference, where all 8 shots were acquired at $R_{inplane}$=8 acceleration per shot.

Bland-Altman analysis[23] was used to assess the accuracy of T2* maps generated by proposed reconstructions. Several ROIs were manually selected for this analysis (Figure 4).

For QSM, tissue phase was estimated using Laplacian unwrapping[24] and V-SHARP[25,26] background removal.

Results & Discussion

Figure 3 shows results from multi-echo multi-shot 3D-BUDA acquisition at $R_{inplane}$=8. Two time-matched acceleration strategies are considered: Sampling 8-shots at R_z=2-fold partition acceleration and 4-shots with full sampling in partition direction (R_z=1). Both joint multi-echo and separate reconstructions for each echo are performed.

When echoes are separately reconstructed, $R_{inplane}\times R_z$=8×2 case using 8-shots has higher reconstruction accuracy (3.90% RMSE) than $R_{inplane}\times R_z$=8×1 with 4-shots (6.14%), due to higher image quality produced by more evenly distributed ky-kz sampling pattern in k-space coverage. Having acquired 8-shots also permitted better B_0 estimation using interim 4-shot blip-up and 4-shot blip-down reconstructions in *topup*, which were "effectively" $R_{inplane}\times R_z$=2×2-fold accelerated and could be readily reconstructed using SENSE.

Joint reconstruction with CAIPI sampling across echoes/shots further improved these results, where 8-shot $R_{inplane}\times R_z$=8×2 yielded 2.25%, and 4-shot $R_{inplane}\times R_z$=8×1 had 5.98% RMSE. As such, the proposed joint multi-echo reconstruction provided >2.5-fold improvement over separate reconstructions.

For T2* mapping, Figure 4 indicates the Bland-Altman analysis comparing 3D-joint-CAIPI-BUDA reconstruction and reference standard multi-echo 3D-GRE data (TA: ~35 minutes). Bland-Altman plots show the mean and difference for the ROIs of T2* values; all values are within the limits of agreement, although some minor biases exist.

Figure 5 displays QSM results from 3D-joint-CAIPI-BUDA ($R_{inplane}\times R_z$=8×2, TA: 47s, 8-shot). Shot-to-shot and echo-to-echo phase variations caused by physiologic variations were effectively removed in the proposed joint-Buda scheme. The conditioning of dipole inversion can be further improved using multi-orientation sampling[27], which is facilitated by the proposed efficient acquisition strategy.

Conclusion

The proposed 3D-joint-CAIPI-BUDA combines staggered CAIPI-sampling across multiple shots, multi-echo acquisition with inverted polarity and joint Hankel structured low-rank reconstruction to boost SNR and eliminate distortion simultaneously. This enables accurate, distortion-free whole-brain T2* mapping and QSM at the resolution of 1.1×1.1×1 mm^3 in 47s.

Acknowledgements

This work was supported by:

NSFC grant (61801205), CPSF grant (2018M633073), the Guangdong Medical Scientific Research Foundation (A2019041) and OCPC fellowship;

NIBIB grants: R01 EB019437, R03 EB031175, R01 EB028797, P41 EB030006, U01 EB026996 and U01 EB025162;

NIMH grants: R01 MH116173;

Shared instrumentation grants S10-RR023401 and S10- RR023043; and NVIDIA GPU grants.

References

1. Gracien RM, Maiworm M, Brüche N, et al. How stable is quantitative MRI? – Assessment of intra- and inter-scanner-model reproducibility using identical acquisition sequences and data analysis programs. *Neuroimage*. 2020;207(August 2019):1-11.

2. van Wijnen A, Petrov F, Maiworm M, et al. Cortical quantitative MRI parameters are related to the cognitive status in patients with relapsing-remitting multiple sclerosis. *Eur Radiol*. 2020;30(2):1045-1053.

3. Larsen B, Olafsson V, Calabro F, et al. Maturation of the human striatal dopamine system revealed by PET and quantitative MRI. *Nat Commun*. 2020;11(1):1-10.

4. Bandettini PA. Twenty years of functional MRI: The science and the stories. *Neuroimage*. 2012;62(2):575-588.

5. Liao C, Cao X, Cho J, Zhang Z, Setsompop K, Bilgic B. Highly efficient MRI through multi-shot echo planar imaging. 2019;1113818(September 2019):43.

6. Cao X, Wang K, Liao C, et al. Efficient T2 mapping with blip-up/down EPI and gSlider-SMS (T2-BUDA-gSlider). *Magn Reson Med*. 2021;86(4):2064-2075.

7. Dierkes T, Neeb H, Shah NJ. Distortion correction in echo-planar imaging and quantitative T2* mapping. *Int Congr Ser*. 2004;1265(C):181-185.

8. Langkammer C, Bredies K, Poser BA, et al. Fast quantitative susceptibility mapping using 3D EPI and total generalized variation. *Neuroimage*. 2015;111:622-630.

9. Ardekani S, Sinha U. Geometric distortion correction of high-resolution 3 T diffusion tensor brain images. *Magn Reson Med*. 2005;54(5):1163-1171.

10. Chen N kuei, Guidon A, Chang HC, Song AW. A robust multi-shot scan strategy for high-resolution diffusion weighted MRI enabled by multiplexed sensitivity-encoding (MUSE). *Neuroimage*. 2013;72:41-47.

11. Jeong HK, Gore JC, Anderson AW. High-resolution human diffusion tensor imaging using 2-D navigated multishot SENSE EPI at 7 T. *Magn Reson Med*. 2013;69(3):793-802.

12. Mani M, Jacob M, Kelley D, Magnotta V. Multi-shot sensitivity-encoded diffusion data recovery using structured low-rank matrix completion (MUSSELS). *Magn Reson Med*. 2017;78(2):494-507.

13. Bilgic B, Poser B, Langkammer, Christian Setsompop K, Liao C. 3D-BUDA Enables Rapid Distortion-Free QSM Acquisition. *Proc 28th Annu Meet ISMRM*. 2020;virtual meeting:596.

14. Breuer FA, Blaimer M, Heidemann RM, Mueller MF, Griswold MA, Jakob PM. Controlled aliasing in parallel imaging results in higher acceleration (CAIPIRINHA) for multi-slice imaging. *Magn Reson Med*. 2005;53(3):684-691.

15. Setsompop K, Gagoski BA, Polimeni JR, Witzel T, Wedeen VJ, Wald LL. Blipped-controlled aliasing in parallel imaging for simultaneous multislice echo planar imaging with reduced g-factor penalty. *Magn Reson Med*. 2012;67(5):1210-1224.

16. Jenkinson M, Beckmann CF, Behrens TEJ, Woolrich MW, Smith SM. FSL. *Neuroimage*. 2012;62:782-790.

17. Jin KH, Lee D, Ye JC. A General Framework for Compressed Sensing and Parallel MRI Using Annihilating Filter Based Low-Rank Hankel Matrix. *IEEE Trans Comput Imaging*. 2016;2(4):480-495.

18. Mani M, Jacob M, McKinnon G, et al. SMS MUSSELS: A navigator-free reconstruction for simultaneous multi-slice-accelerated multi-shot diffusion weighted imaging. *Magn Reson Med*. 2020;83(1):154-169.

19. Samsonov AA, Kholmovski EG, Parker DL, Johnson CR. POCSENSE: POCS-based reconstruction for sensitivity encoded magnetic resonance imaging. *Magn Reson Med*. 2004;52(6):1397-1406.

20. Ma D, Gulani V, Seiberlich N, et al. Magnetic resonance fingerprinting. *Nature*. 2013;495(7440):187-192.

21. Polak D, Chatnuntawech I, Yoon J, et al. Nonlinear dipole inversion (NDI) enables robust quantitative susceptibility mapping (QSM). *NMR Biomed*. 2020;33(12):1-13.

22. Milovic C, Shmueli K. Automatic , Non-Regularized Nonlinear Dipole Inversion for Fast and Robust Quantitative Susceptibility Mapping. *Proc 29th Annu Meet ISMRM, virtual Meeting*. Published online 2021:3982.

23. D. G. ALTMAN, J. M. BLAND. Measurement in Medicine: the Analysis of Method Comparison Studies. *Stat*. 1983;32(7):307-317.

24. Li W, Wu B, Liu C. Quantitative susceptibility mapping of human brain reflects spatial variation in tissue composition. *Neuroimage*. 2011;55(4):1645-1656.

25. Wu B, Li W, Guidon A, Liu C. Whole brain susceptibility mapping using compressed sensing. *Magn Reson Med*. 2012;67(1):137-147.

26. Schweser F, Sommer K, Deistung A, Reichenbach JR. Quantitative susceptibility mapping for investigating subtle susceptibility variations in the human brain. *Neuroimage*. 2012;62(3):2083-2100.

27. Liu T, Spincemaille P, De Rochefort L, Kressler B, Wang Y. Calculation of susceptibility through multiple orientation sampling (COSMOS): A method for conditioning the inverse problem from measured magnetic field map to susceptibility source image in MRI. *Magn Reson Med*. 2009;61(1):196-204.

Figures

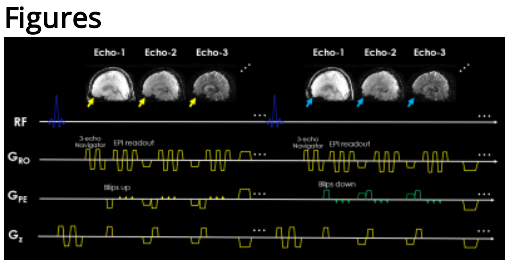

FIG.1. 3D-BUDA multi-shot multi-echo sequence schematic. 3D slab-selective EPI data were acquired using a complementary blip-up /down acquisitions multi-shot EPI with frequency-selective fat suppression. Blip up/down were implemented for each echo (see yellow and green blips in phase encoding gradient), respectively. Subsequently, followed by a rewinder gradient before the next echo.

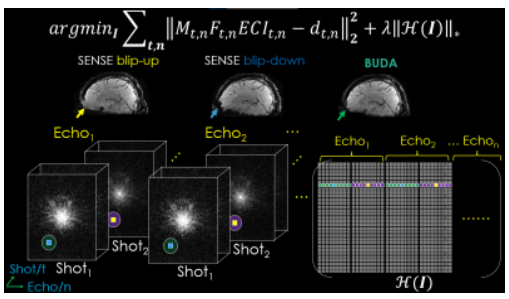

FIG.2. The proposed 3D-joint-BUDA image reconstruction framework for multi-shot multi-echo GRE-EPI data. For joint image reconstruction, the new Hankel matrix is constructed using the neighborhood along both echo and shot dimensions of the GRE-EPI dataset.

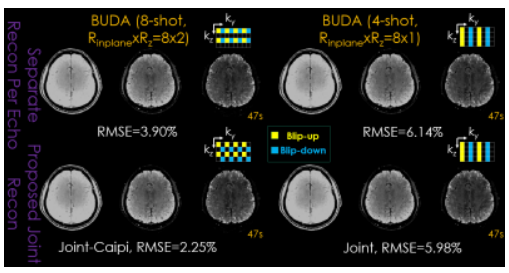

FIG.3. Comparison of different approaches with different sampling patterns (upper right corner of each subpart) on image quality for 3D-BUDA dataset with the same sampling amount (TA: 47s). First column: conventional 8-shot without and with CAIPIRINHA sampling. Second column: conventional 4-shot Rz = 1 without and with joint structured low-rank reconstruction. Three columns in each part are the three echoes of 3D-BUDA imaging, respectively.

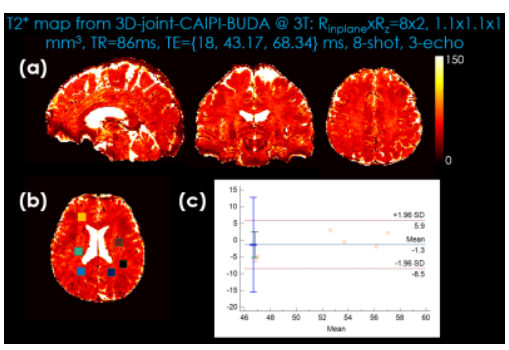

FIG.4. Comparison of the Bland-Altman plots displaying the mean and difference of T2* mapping generated by 3D-joint-CAIPI-BUDA image reconstruction and standard multi-echo GRE. (a) T2* mapping generated by 3D-joint-CAIPI-BUDA (8-shot, $R_{inplane}xR_Z$=8x2). (b) Selected regions of interest. (c) 3D-joint-CAIPI-BUDA (Rinplane=8, Rz=2, 8-shot) vs. standard multi-echo GRE (mean: GRE-51.58 vs. 3D-joint-CAIPI-BUDA-52.88).

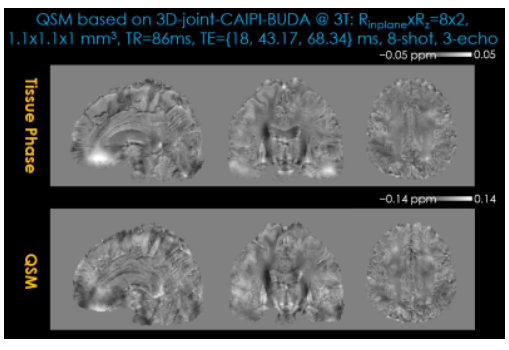

FIG.5. Tissue phase (first row) and quantitative susceptibility mapping (second row) results estimated using 3D-joint-CAIPI-BUDA image reconstruction (Reduction factor: $R_{inplane}$=8, Rz=2, TA=47s). The local tissue phase was obtained by Laplacian unwrapping and V-SHARP filtering (10 mm largest kernel size).